COMMON CAROTID ARTERY WALL LOCALIZATION IN B-MODE ULTRASOUND IMAGES

Jan Dorazil
Doctoral Degree Programme (2), FEEC BUT
E-mail: xdoraz04@stud.feec.vutbr.cz

Supervised by: Kamil Říha
E-mail: rihak@feec.vutbr.cz

Abstract: Analysis of B-mode ultrasound images capturing the common carotid artery (CCA) provides significant indicators of the overall health of the cardiovascular system. In this paper we propose a novel method for automatic localization of the artery wall contour (approximated by circle) in utrasound images of the transverse section of the CCA. After detection of a region of interest (ROI) using a modified Viola-Jones detector we localize the best-fitting circle, which delimits the artery wall contour, by exhaustive search. Experimental results on a dataset of 145 ultrasound images show that the method outperforms a reference method based on the Hough transform and presents an excellent robustness against additive noise on different SNR levels.

Keywords: common carotid artery, B-mode ultrasound, artery wall localization.

1 INTRODUCTION

Carotid ultrasound examination have become a widely used method for prevention of cardiovascular diseases, quantification of artery stenosis and characterization of the artery wall plaque, mainly due to its non-invasive nature and good availability [1]. The most notable examples of examination techniques, relevant in ultrasound images, are currently based either on segmentation of the common carotid artery (CCA) [2], [3], yielding an estimate of the intima-media thickness, or CCA motion tracking techniques [4, 5, 6], which can be used to evaluate the dynamical properties of the artery. Currently most of the techniques, however, require manual initialization, where the initial location of the artery conotur is given by the user. This leads to variations in the initial contour and consequently to inconsistent precision of the segmentation or tracking method. Some examples of automatic artery wall localization methods can, however, be found in the literature.

When considering only methods designed for B-mode ultrasound images of the CCA transverse section, which is the main objective of this paper, we find [7], where a method for detection of the CCA wall based on Hough transform is proposed. The computational complexity of this methods is high, because the parametric space of the Hough transform needs to cover the whole image domain. Furthermore variations in the artery shape and presence of acoustic artifacts [8] inhibit the methods performance. In [9] the authors propose a grammar-guided genetic programming based method. In [10] a method based on modified Viola-Jones detector is proposed, outperforming [9] in terms of detection success rate. This method, however, provides only a rectangular region of interest (ROI), delimiting the area of the CCA transverse section. In [4] the authors develop an extension of [10] by employing the Hough transform for localization of the CCA wall contour after ROI detection. Significantly decreased parametric space of the Hough transform then allows for real-time processing. As a result of the mentioned methods we generally obtain a circle approximately labeling the CCA wall.

In this paper, we present a robust CCA wall localization method improving on [4]. After ROI detection we perform a circle localization by maximization of a particular criterion by exhaustive search

over all possible circles in ROI. On a dataset of 145 ultrasound images, including challenging cases with low contrast and deformations, we show that our method outperforms the reference method of [4]. Finally we demonstrate the robustness of the proposed method on ultrasound images with additive noise of different signal to noise ratios (SNR).

2 METHODS

The proposed method is based on the following processing chain. As a first step we detect a ROI, which delimits a rectangular area of the CCA transverse section. The pixel intensities of the image portion delimited by the ROI are then normalized in order to improve contrast and supress high intensity peaks, which might confuse the following circle localization algorithm. On the detected ROI, we then perform an exhaustive search over all possible CCA circle center points and radii. The circle that maximizes a particular criterion represents the final estimate.

2.1 ROI DETECTION

In this step we detect the ROI which delimits a rectangular area of the ultrasound image where the CCA transverse section lays. This is done by the modified Viola-Jones algorithm proposed in [10]. Further processing is done on the ROI, which significantly decreases the computational complexity.

2.2 INTENSITY NORMALIZATION

The success of the circle detection step is strongly dependent on the image intensities. We therefore developed an intensity normalization technique taking inspiration from [11]. Using Otsu's method [12] we calculate a threshold τ separating image intensities into two classes: one representing the highly echogenic tissues of the artery wall and the other representing blood and low echogenic tissues. Our objective is now to ensure that the threshold between the two classes is matched in all processed images. This can be achieved by remapping the image intensities by a function $g(\cdot)$ which meets the following criteria (assuming that image intensities lay in the range $[0,255]$): $g(0) = 0$, $g(\tau) = \tau'$, $g(255) = 255$, where $\tau' \in (0,255)$ is a constant defining the target threshold value. In the proposed method we use the monotone piecewise cubic function [13] which meets the specified criteria, while having the smoothness property over the whole domain. This function, moreover, has the desirable property of monoticity which ensures that the pixel order, as sorted by its intensities, remains the same after normalization. In Figure 1 we present a remapping function whose parameters are determined from a real ultrasound image, which is depicted before and after intensity normalization.

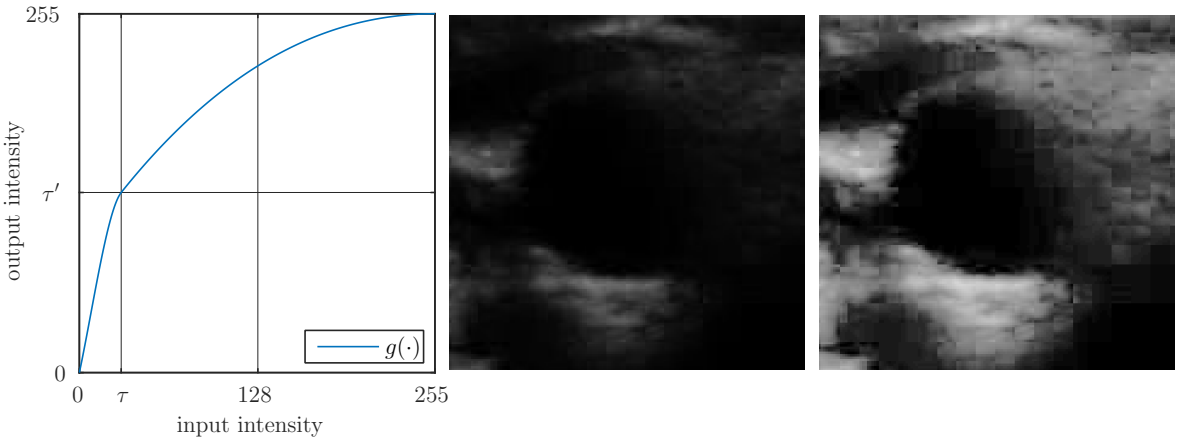

Figure 1: Example remapping function $g(\cdot)$ (left), image before intensity normalization (middle), image after intensity normalization (right).

2.3 CIRCLE LOCALIZATION

The general algorithm for circle localization can be described as follows. We iterate through all combinations of circle center point coordinates $x \in [X_\mathrm{l}, X_\mathrm{h}]$, $y \in [Y_\mathrm{l}, Y_\mathrm{h}]$ and radii $r \in [R_\mathrm{l}, R_\mathrm{h}]$. The limits X_l, X_h, Y_l and Y_h are given by the ROI, while the limits R_l and R_h are given a priori from our anatomical knowledge and properties of the imaging system. Here R_l and R_h are given as the smallest and largest possible CCA radius respectively (in pixels). For each circle we calculate the average intensity of pixels laying inside the circle μ_in and on the circle boundary μ_on. The thickness of the circle boundary (in pixels) is given by a constant b. Circle which maximize the difference $\mu_\mathrm{on} - \mu_\mathrm{in}$ is the final estimate of the proposed method. Obviously a fast implementation of the algorithm can be developed by means of convolution (in spatial or frequency domain) with an appropriately designed convolution kernel for each radius r.

In order to reduce the computational complexity we developed a multiscale implementation of the algorithm. The circle localization is first performed on a version of the original image decimed by a factor $s < 1$. The resulting circle center point $(x_\mathrm{m}\ y_\mathrm{m})^T$ and radius r_m is then used to derive new search limits as

$$X'_\mathrm{l} = \lfloor X \rfloor, \quad X'_\mathrm{h} = \lceil X + d \rceil, \quad Y'_\mathrm{l} = \lfloor Y \rfloor, \quad Y'_\mathrm{h} = \lceil Y + d \rceil, \quad R'_\mathrm{l} = \lfloor R \rfloor, \quad R'_\mathrm{h} = \lceil R + d \rceil,$$

where $X \triangleq \frac{x_m}{s}$, $Y \triangleq \frac{y_m}{s}$, $R \triangleq \frac{r_m}{s}$ and $d \triangleq \frac{1}{2s}$. The circle localization algorithm is then repeated on the original image with the new set of limits, obtaining the final circle estimate.

3 RESULTS AND DISCUSSION

To demonstrate the performance of our method we utilized a dataset (denoted as S_∞) of 145 ultrasound images of a healthy patient. The images were acquired by Ultrasonix OP with a linear probe L14–5/38 (Ultrasonix Medical, Richmond, BC, Canada) at a frequency of 7,5MHz. The dataset contains also challenging images with low contrast and deformations caused by tilting of the hand-held probe. Moreover, we created two more datasets S_{25} and S_{15} by superimposing 50 realizations of additive zero-mean Gaussian noise to images of dataset S_∞. In the first case (S_{25}) the SNR is 25dB and in the second case (S_{15}) the SNR is 15dB. For each image of the dataset S_∞ (naturally also for S_{25} and S_{15}) a manual segmentation is available which serves as the ground-truth for performance evaluation. In the following text we will refer to the outline of the manual segmentation as the "true contour".

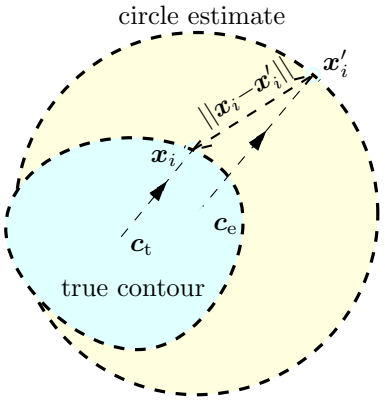

Figure 2: Geometry used in calculation of ε.

The precision of an estimated circle is evaluated by an error metric ε [px] which quantifies the mean distance of each point on the true contour to the circle. The error metric is calculated as follows. First we calculate the center of gravity $\mathbf{c}_\mathrm{t}$ of the area outlined by the true contour. Then we iterate through each pixel $\mathbf{x}_i$ of the true contour, calculating the vector $\delta_i \triangleq \mathbf{x}_i - \mathbf{c}_\mathrm{t}$. A corresponding point $\mathbf{x}'_i$ on the estimated circle with center $\mathbf{c}_\mathrm{e}$ is then found at intersection of the half-line $q\delta_i + \mathbf{c}_\mathrm{e}$, where $q > 0$, with the circle outline. The metric ε is then calculated as the arithmetic mean of the distance between all corresponding points $\mathbf{x}_i$ and $\mathbf{x}'_i$, i.e.,

$$\varepsilon \triangleq \frac{1}{N} \sum_{i=1}^{N} ||\mathbf{x}_i - \mathbf{x}'_i||,$$

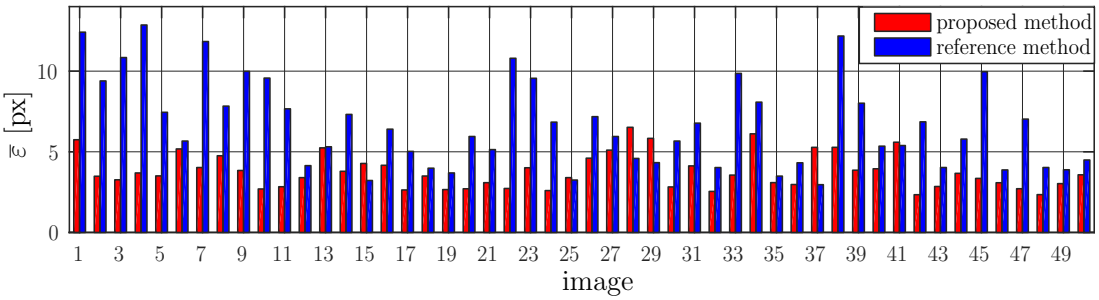

Figure 3: Ensemble mean error evaluated for the first 50 images of the dataset S_{15}.

	Proposed method			Reference method		
Dataset	S_∞	S_{25}	S_{15}	S_∞	S_{25}	S_{15}
Mean error [px]	3,99	4,12	4,12	6,75	6,90	7,87
Misdetection rate [%]	0,69	0,74	1,38	2,76	3,05	5,57

Table 1: Mean error and misdetection rates of the proposed and reference method.

where N denotes the number of pixels of the true contour. The discussed geometry is depicted in Figure 2. In the following text we assume that a value of ε larger that 30px indicates a misdetection.

For all three datasets we evaluated the *mean error* as the arithmetic mean of ε over all 145 images, and all 50 noise realizations (in case of S_{25} and S_{15}). Misdetections (i.e. values of $\varepsilon > 30$px) are excluded from the mean error calculation and the number of misdetections is accumulated in order to obtain the *misdetection rates*, i.e. the percentual proportion of missed detections against the number of all detections. The obtained values of mean error and misdetection rates are listed in Table 1. One can see that the proposed method ourperforms the reference method on all three datasets. The advantage in performance of the proposed method gets more pronounced with decreasing SNR. The excellent performance in scenarios with low SNR can be attributed to the spatial smoothing—an implicit part of the localization algorithm. For the first 50 images of dataset S_{15} we evaluated the *ensemble mean error* $\bar{\varepsilon}$, defined as the arithmetic mean of ε over all noise realizations. The obtained values are presented in Figure 3.

In all experiments we utilized the following parameter set: $\tau' = 195$, $R_l = 20$px, $R_h = 50$px, $b = 2$px and $s = 0{,}3$. The multiscale, convolution based implementation has in average a running time of 24ms per one image on Intel Core i5-7500 CPU with base frequency of 3,40GHz.

4 CONCLUSION

We proposed a robust method for localization of the artery wall (approximated by a circle) in B-mode ultrasound images capturing the transverse section of the common carotid artery (CCA). After region of interest (ROI) detection we localize the CCA wall by exhaustive search through all possible circle center and radius combinations inside the ROI. Experimental evidence demonstates that the proposed method outperforms a reference method, based on the Hough transform, in terms of precision and misdetection rates. Note that the simplest possible criterion (i.e. the difference between two mean intensities) was used to choose the best-fitting circle. The size of the ROI (about 132×132px), however, allows for a more sophisticated criterion to be designed while still keeping the computational complexity acceptable.

ACKNOWLEDGEMENT

This work was supported in part by the Czech Science Foundation (GACR) under Grant 17 19638S and by the Czech National Sustainability Programme under Grant LO1401. For the research, infrastructure of the SIX Center was used.

REFERENCES

[1] A. Lorenzová, "Carotid ultrasound in primary and secondary prevention of stroke," *Cor Vasa*, vol. 58, no. 2, pp. 273–278, Apr. 2016.

[2] J. Stoitis, S. Golemati, S. Kendros, and K. S. Nikita, "Automated detection of the carotid artery wall in B-mode ultrasound images using active contours initialized by the Hough Transform," in *Conf. Proc. IEEE Eng. Med. Biol. Soc.*, Vancouver, BC, Canada, Aug. 2008, pp. 3146–3149.

[3] X. Yang et al., "Ultrasound Common Carotid Artery Segmentation Based on Active Shape Model," *Comput. Math. Methods Med.*, vol. 2013, no. 345968, Mar. 2013.

[4] K. Říha, M. Zukal, and F. Hlawatsch, "Analysis of Carotid Artery Transverse Sections in Long Ultrasound Video Sequences," *Ultrasound Med. Biol.*, vol. 44, no. 1, pp. 153–167, Jan. 2018.

[5] Z. Gao, Y. Li, Y. Sun, J. Yang, H. Xiong, H. Zhang, X. Liu, W. Wu, D. Liang, and S. Li, "Motion tracking of the carotid artery wall from ultrasound image sequences: a nonlinear state-space approach," *IEEE Trans. Med. Imag.*, vol. 37, no. 1, pp. 273–283, Jan. 2017.

[6] A. Gastounioti, N. N. Tsiaparas, S. Golemati, J. S. Stoitsis, and K. S. Nikita, "Affine optical flow combined with multiscale image analysis for motion estimation of the arterial wall from B-mode ultrasound," in *Proc. Ann. Int. Conf. IEEE Eng. Med. Biol. Soc.*, Boston, MA, USA, Aug. 2011, pp. 559–562.

[7] S. Golemati, J. Stoitsis, E. G. Sifakis, T. Balkizas, and K. S. Nikita, "Using the Hough Transform to Segment Ultrasound Images of Longitudinal and Transverse Sections of the Carotid Artery," *Ultrasound Med. Biol.*, vol. 33, no. 12, pp. 1918–1932, Jul. 2007.

[8] F. W. Kremkau and K. J. Taylor, "Artifacts in ultrasound imaging," *J. Ultrasound Med.*, vol. 5, no. 4, pp. 227–237, Apr. 1986.

[9] R. Beneš, J. Karásek, R. Burget, and K. Říha, "Automatically designed machine vision system for the localization of CCA transverse section in ultrasound images," *Comput. Methods Programs Biomed.*, vol. 109, no. 1, pp. 92–103, Jan. 2013.

[10] K. Říha, J. Mašek, R. Burget, R. Beneš, and E. Závodná, "Novel method for localization of common carotid artery transverse section in ultrasound images using modified Viola-Jones detector," *Ultrasound Med. Biol.*, vol. 39, no. 10, pp. 1887–1902, Oct. 2013.

[11] Y. Omran, R. Beneš, and K. Říha, "Suitable Image Intensity Normalization for Arterial Visualization," *Int. J. Adv. Telecommun. Electrotech. Signals Syst.*, vol. 1, no. 2–3, pp. 53–56, Dec. 2012.

[12] N. Otsu, "A Threshold Selection Method from Gray-Level Histograms," *IEEE Trans. Syst. Man. Cybern.*, vol. 9, no. 1, pp. 62–66, Jan. 1979.

[13] F. N. Fritsch and R. E. Carlson, "Monotone Piecewise Cubic Interpolation," *SIAM J. Numer. Anal.*, vol. 17, no. 2, pp. 238–246, Apr. 1979.